Materials Letters 255 (2019) 126551

Contents lists available at ScienceDirect

Materials Letters

journal homepage: www.elsevier.com/locate/mlblue

Production of PMMA-based nanocellular polymers using low demanding saturation conditions

Victoria Bernardo *, Judith Martín-de León, Miguel Ángel Rodríguez-Pérez

Cellular Materials Laboratory (CellMat), Condensed Matter Physics Department, University of Valladolid, Campus Miguel Delibes, Paseo de Belén n°7, 47011 Valladolid, Spain

ARTICLE INFO

Article history:
Received 12 June 2019
Received in revised form 11 August 2019
Accepted 15 August 2019
Available online 16 August 2019

Keywords:
Nanocellular polymer
Nanocellular foam
Gas dissolution foaming
PMMA

ABSTRACT

Nanocellular polymers are novel materials characterized by nanometric cell sizes with huge potential in many industrial applications. However, their production is challenging and usually requires demanding processing conditions that make difficult the production at industrial scale. In this work, we prove that nanocellular polymers based on PMMA can be obtained, thanks to the addition of nucleating species, using low saturation pressure (6 MPa) and room saturation temperature in a gas dissolution foaming process. Nanoparticles and block copolymers at different concentrations are used to obtain a collection of nanocellular polymers with densities ranging 0.16–0.58 and cell sizes from 120 to 900 nm. Comparison with the literature results shows that the processing parameters used in this work are the less demanding ever used for producing nanocellular PMMA.

1. Introduction

Nowadays, the use of cellular polymers is extremely widespread in almost every sector, such as automotive, leisure or packaging, among others [1,2]. Due to their technological relevance in many applications, the development of new and advanced cellular polymers is always a priority field of research in this area. The next generation of cellular polymers are the so-called nanocellular polymers, characterized by cell sizes from tens to hundreds of nanometers. The relevance of these materials lies in their interesting properties [3], such as their reduced thermal conductivity [4–6], improved mechanical properties [7,8], the possibility of producing transparent nanocellular polymers [9,10], their interesting dielectric and acoustic properties [11,12] and their high surface area [13].

One of the key challenges in the field of nanocellular polymers is the production of these materials using facile and scalable-up production routes. The most extended fabrication process for nanocellular polymers is the so-called gas dissolution foaming [14], developed in the 1980s with the invention of microcellular polymers [15]. However, the evolution from microcellular polymers to nanocellular materials implies a significant increase in the nucleation density, from 10^9 to 10^{13} nuclei/cm^3, so the complexity of the process increases accordingly. Currently, there are two main approaches to produce nanocellular polymers. The first one is the use of processing conditions that maximize the amount of gas absorbed in the sample, and thus the nucleation. High saturation pressures [16,17] or low saturation temperatures [18,19] allow reaching the high solubilities needed to produce nanocellular polymers. However, these conditions complicate the possible industrial production. Another possibility is the use of nucleating species to promote nucleation [20,21], and in this case, mild processing conditions can be used.

In this work, we have produced nanocellular poly(methyl methacrylate) (PMMA) using low pressure (6 MPa) and room temperature as saturation conditions, using two different nucleating agents: sepiolite nanoparticles and MAM (poly(methyl methacrylate)-poly(butyl acrylate)-poly(methyl methacrylate)) block copolymer. Nanometric cell sizes from 120 to 900 nm are obtained. To our knowledge, only in the work of Liu and coworkers [22] there are some previous studies with similar conditions. Working at 5.5 MPa and room temperature, they obtained foamed films of PMMA with 400 nm of cell size and relative density 0.32 by adding nanosilica particles with a poly(dimethylsiloxane) (PDMS) shell. Apart from that paper, all the PMMA-based nanocellular materials reported in the literature are produced at higher pressures and/or lower temperature [23]. Then, this is the first time that bulk nanocellular polymers (i.e., samples of several millimeters thick) based on PMMA are produced using such a low pressure (6 MPa) with saturation at room temperature. Our work aims at paving the way for future studies in the implementation of the gas dissolution foaming process at industrial scale to produce nanocellular parts to be used in real applications.

* Corresponding author.
E-mail address: vbernardo@fmc.uva.es (V. Bernardo).

https://doi.org/10.1016/j.matlet.2019.126551
0167-577X/

2. Experimental

2.1. Materials

PMMA V825T (M_n = 43 kg/mol, M_w = 83 kg/mol) was kindly supplied by ALTUGLAS® International. Sepiolites (needle-like magnesium silicate nanoparticles [24]) modified with a quaternary ammonium salt (SQAS) [25] were kindly provided by Tolsa S.A (Spain). Several MAM block copolymers: Nanostrength M51 (M_n = 25 kg/mol, M_w = 46 kg/mol, 48 wt% of PBA), Nanostrength M52 (M_n = 44 kg/mol, M_w = 75 kg/mol, 52 wt% of PBA) and Nanostrength M53 (M_n = 82 kg/mol, M_w = 128 kg/mol, 54 wt% of PBA) [26] were kindly supplied by Arkema. These MAM grades would be referred from now on as L, M and H, respectively (low, medium and high molecular weight). Medical grade CO_2 (99.9% purity) was used as the blowing agent.

2.2. Solid blends production

Various nanocomposites of PMMA/Sepiolites and PMMA/MAM binary blends were produced (see the different samples fabricated in Table 1). The raw PMMA and the selected filler (sepiolites or MAM) in the desired proportions were melt-blended with a twin-screw extruder COLLIN TEACH-LINE ZK 25T (L/D = 24, screw diameter = 25 mm). The materials were first dried in vacuum at 50 °C overnight. The temperature profile varied from 160 °C to 200 °C, and the screw speed was 40 rpm. The extruded material was cooled in a water bath and pelletized. After drying, each formulation was extruded again under the same conditions. Then, the pelletized formulations were compressed molded into 4 mm thick solid sheets using a hot press (Talleres Remtex, Barcelona). The temperature in the press was 250 °C. During 8.5 min, the pellets were heated, and then a constant pressure of 17 MPa was applied during one minute at the same temperature. Then the samples were cooled down using the same pressure. From the solid sheets, samples of $20 \times 10 \times 4\ mm^3$ were cut for the foaming experiments. Note that pure PMMA was processed with the same conditions to be used as reference material.

2.3. Gas dissolution foaming experiments

The foaming experiments were performed using a high-pressure vessel (PARR 4681, Parr Instrument Company). Pressure can be controlled with a pressure pump controller (SFT-10, Supercritical Fluid Technologies Inc). A clamp heater of 1200W and a CAL 3300 temperature controller allow the control of the temperature. A two-step foaming process was used [14]. The samples were put into the pressure vessel at a CO_2 pressure of 6 MPa and a temperature of 25 °C for the saturation stage during 72 h to assure saturation (this time was overestimated from the data of [27] at similar conditions). At these conditions, pure PMMA absorbs around 22 wt% of CO_2. Then, the pressure was abruptly released (pressure drop rate: 0.7 MPa/s). Finally, the samples were removed from the vessel and introduced into a thermal bath for 2 min for foaming. The foaming temperature, T_{foam}, was optimized for every system to achieve the maximum expansion (Table 1). The time between the release of the pressure and the immersion of the samples in the bath was 3.5 min.

2.4. Characterization

The density of the solids (ρ_s) was measured with a gas pycnometer (AccuPyc II 1340, Micromeritics). The density of the cellular materials (ρ) was determined with the water-displacement method based on the Archimedes' principle using a density determination kit for an AT261 Mettler-Toledo balance. More than 200 μm of the surface of cellular samples were removed with a polisher (LaboPOl2-LaboForce3, Struers) before measuring the densities. Relative density is defined as $\rho_r = \rho/\rho_s$.

The samples were fractured by cooling them in liquid nitrogen for visualization and coated with gold using a sputter coater (SCD 005, Balzers Union). The surface morphology was analyzed using an ESEM Scanning Electron Microscope (QUANTA 200 FEG). The materials with sepiolites present a bimodal structure with micro and nanometric cells, and the relative volume occupied by the population of nanometric cells, V_{nano}, was measured to quantify the bimodality. The PMMA/MAM samples and the nanometric population in the PMMA/Sepiolites samples was characterized using a self-developed tool in ImageJ/FIJI [28]. The average cell size, ϕ, and the standard deviation of the cell size distribution, SD, were determined. The parameter SD/ϕ was calculated as an indicator of the homogeneity of the structure. The cell nucleation density N_0 was measured using Kumar's approach [14].

3. Results

Table 1 collects the main characteristics of the materials produced in this work. Note that at these conditions the reference PMMA (samples 1–3, Table 1) are microcellular. Fig. 1 shows the cellular structure of the samples based on PMMA/MAM (samples

Table 1
Characteristics of the materials produced in this work at 6 MPa and 25 °C (foaming time equal to 2 min for all the samples). Samples 1–3: Reference PMMA; Samples 4–9: PMMA/MAM; Samples 10–16: PMMA/Sepiolites.

#	Sample	Filler type	Filler content (wt%)	T_{foam}(°C)	ρ_r	V_{nano}(%)	N_0(nuclei/cm^3)	ϕ(nm)	$\frac{SD}{\phi}$
1	PMMA_80C	–	0	80	0.277	0	$9.0 \cdot 10^{10}$	3360	0.79
2	PMMA_90C	–	0	90	0.197	0	$1.4 \cdot 10^{11}$	3490	0.68
3	PMMA_100C	–	0	100	0.152	0	$1.4 \cdot 10^{11}$	3610	0.81
4	0.1%-L	MAM L	0.1	100	0.157	100	$1.3 \cdot 10^{13}$	872	0.45
5	0.1%-M	MAM M	0.1	100	0.211	100	$9.9 \cdot 10^{13}$	308	0.43
6	0.1%-H	MAM H	0.1	100	0.270	100	$2.6 \cdot 10^{14}$	248	0.41
7	10%-L	MAM L	10	80	0.361	100	$1.4 \cdot 10^{14}$	253	0.74
8	10%-M	MAM M	10	80	0.500	100	$6.9 \cdot 10^{14}$	138	0.48
9	10%-H	MAM H	10	80	0.578	100	$8.2 \cdot 10^{14}$	122	0.45
10	0.5%-SQAS	SQAS	0.5	100	0.162	70	$3.7 \cdot 10^{13}$	582	0.52
11	1%-SQAS	SQAS	1	100	0.207	84	$7.6 \cdot 10^{13}$	415	0.51
12	1.5%-SQAS	SQAS	1.5	90	0.222	78	$5.6 \cdot 10^{13}$	430	0.56
13	2%-SQAS	SQAS	2	90	0.248	84	$8.3 \cdot 10^{13}$	357	0.55
14	3%-SQAS	SQAS	3	90	0.245	90	$1.3 \cdot 10^{14}$	305	0.68
15	5%-SQAS	SQAS	5	90	0.255	77	$2.1 \cdot 10^{14}$	255	0.71
16	10%-SQAS	SQAS	10	90	0.299	52	$3.9 \cdot 10^{14}$	191	0.63

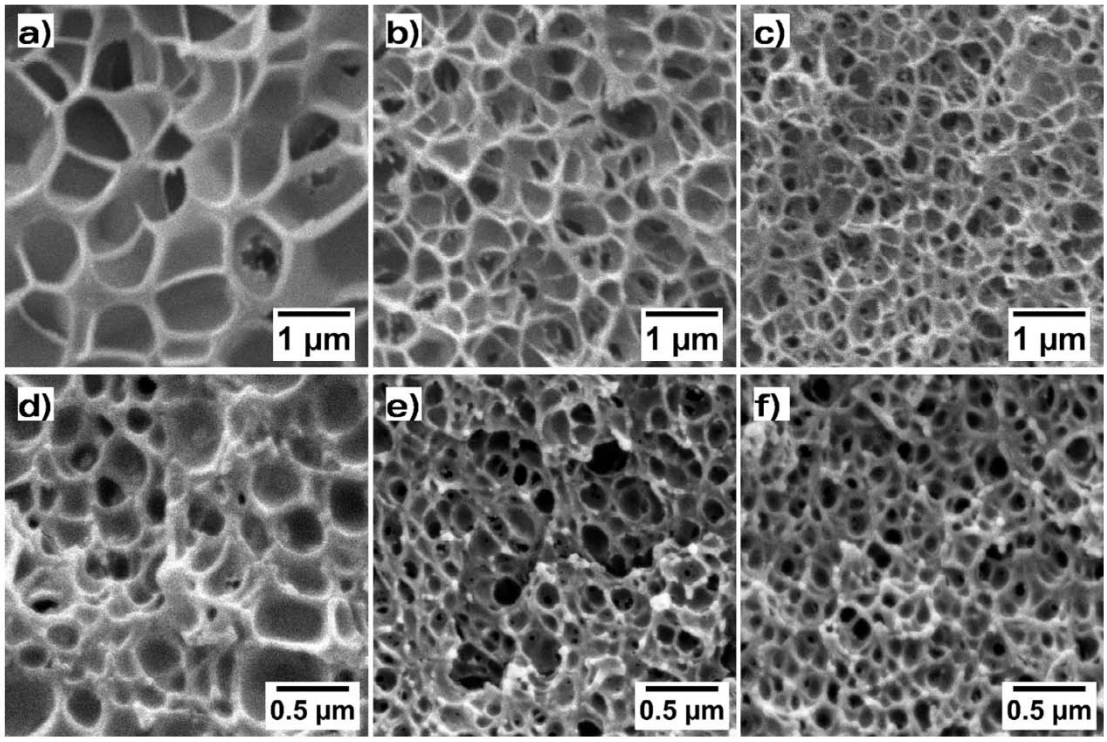

Fig. 1. SEM micrographs of the PMMA/MAM nanocellular samples: a) Sample 4 (0.1%-L), b) Sample 5 (0.1%-M), c) Sample 6 (0.1%-H), d) Sample 7 (10%-L), e) Sample 8 (10%-M) and f) Sample 9 (10%-H).

4–9). Nanocellular samples with cell sizes from 250 to 120 nm are obtained with 10 wt% of MAM, whereas 0.1 wt% of MAM produces higher cell sizes but with lower densities. Fig. 2 shows the micrographs of some of the samples of PMMA/Sepiolites. The addition of sepiolites causes a bimodal cellular structure with micrometric pores due to the particle aggregates [29] (first row of Fig. 2), while the well-dispersed sepiolites produce nanocellular pores (second row of Fig. 2). The parameters N_0 and ϕ in Table 1 correspond to the analysis of the nanocellular region. The fraction occupied by the nanometric pores is higher than 70% for all the materials except for the 10%-SQAS (sample 16) that this value is only 52% because of the big particle aggregates in this system.

The nucleation mechanism taking place in these systems differ depending on the nature of the nucleating agent. On the one hand, in the PMMA/Sepiolites samples, the nucleation takes place in the interface between the particle and the polymer. However, the PBA

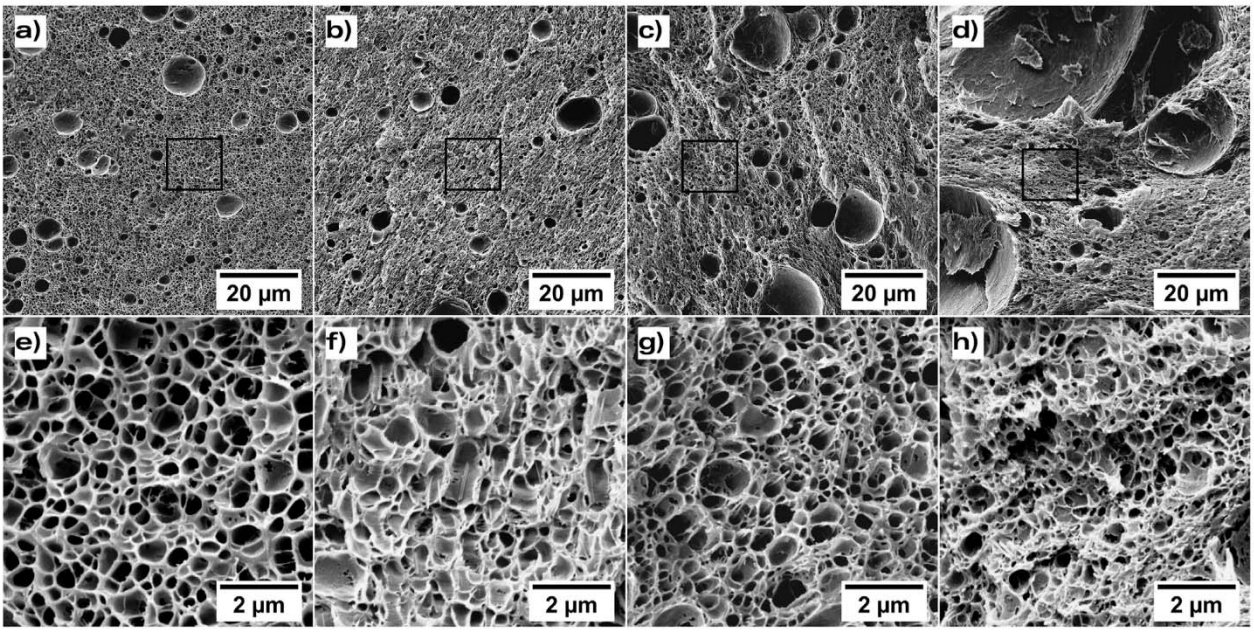

Fig. 2. SEM micrographs of some of the PMMA/Sepiolites bimodal nanocellular samples: a-e) Sample 11 (1%-SQAS), b-f) Sample 14 (3%-SQAS), c-g) Sample 15 (5%-SQAS), d-h) Sample 16 (10%-SQAS). Second row corresponds to zoomed images of the first row.

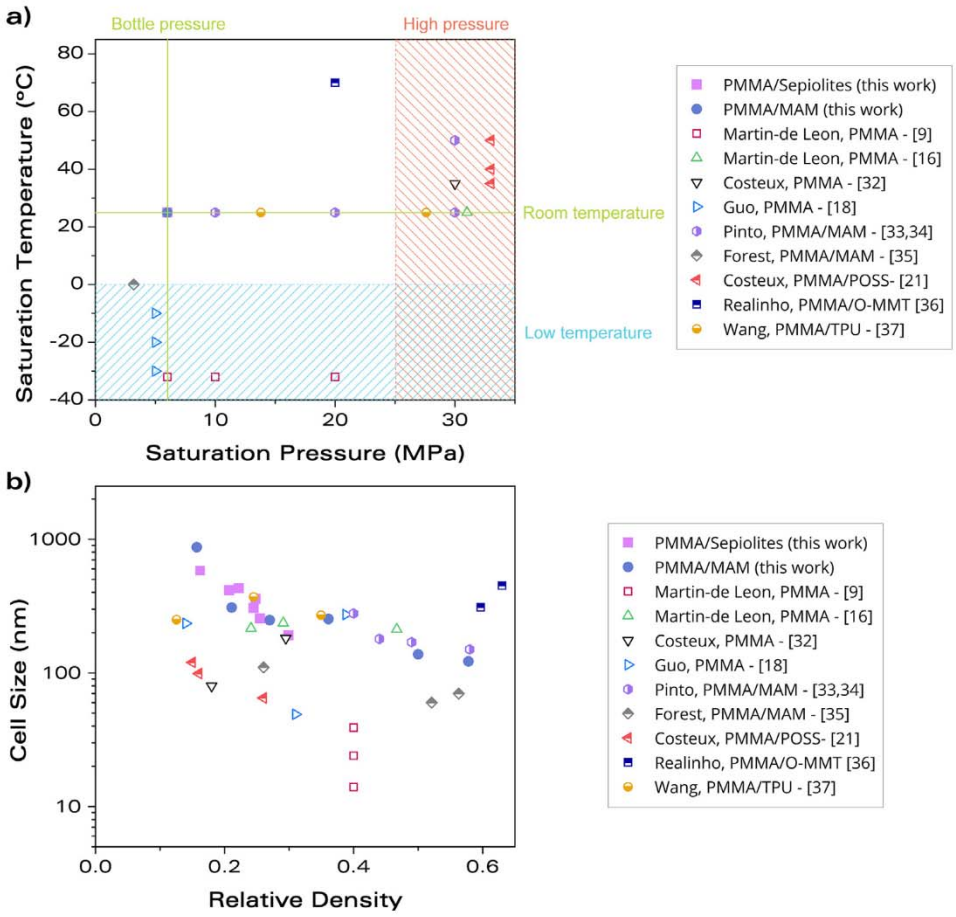

Fig. 3. a) Saturation temperature – saturation pressure, and b) cell size – relative density maps comparing some of the most interesting results from the literature with the materials produced in this work.

block in the MAM copolymer is CO_2-philic and it has a lower glass transition temperature than the PMMA, so in the PMMA/MAM systems the nucleation is promoted in the MAM phase. At 10 wt% of MAM, nucleation takes place in the MAM micelles. As the fraction of MAM is reduced to 0.1 wt% there are no micelles, but still the nucleation occurs in the CO_2-philic MAM molecules. A schematic view of foaming process with these nucleating agents can be found in the Supporting Information.

So far, the structures presented are not so different of other results with these very same systems [26,29–31]. Reducing the amount of MAM reduces density but increases the cell size [30], whereas a higher MAM molecular weight also causes smaller cells and higher nucleation densities [26]. Regarding the sepiolites, the use of higher particle contents reduces the cell size in the nanocellular region because there are more well-dispersed particles [29], but the fraction of nanometric pores is reduced because there are also more micron-sized aggregates [31].

The main novelty of this work lies in the processing conditions used to produce these materials. Fig. 3.a shows a map the processing conditions (saturation pressure and temperature) used in various works from the literature (references [9,16,18,21,32–37]) compared to the parameters used in this paper. All the systems selected for this comparison are based on PMMA as the polymer matrix. Fig. 3.b presents the cell size and relative densities of the samples of this work and those extracted from the bibliography. Those samples with small cell sizes (<100 nm, Fig. 3.b) are produced using either high saturation pressure or extremely low saturation temperatures (Fig. 3.a). Meanwhile, the materials of this work are obtained at room temperature and using a very low pressure of 6 MPa, that is, the pressure of the bottle of gas. Therefore, it is not necessary to use a pressure pump or a heating system during the saturation stage to obtain these materials. We believe that this production conditions could be generalized to other PMMA-based systems containing other nucleating agents with similar characteristics, such as silica nanoparticles [22].

4. Conclusions

Nanocellular polymers based on PMMA filled with different additives were produced using low pressure and room temperature as saturation conditions. Cell sizes in the range from 120 to 900 nm with relative densities of 0.16–0.58 were obtained with this approach.

Two systems able to produce nanocellular polymers based on heterogeneous nucleation were used. First, PMMA nanocomposites with nanometric sepiolites, that allowed producing bimodal cellular structures with a high fraction (>50%) of nanometric pores. The increase of the sepiolite concentration increases the nucleation and reduces the cell size. Second, PMMA/MAM blends, with three MAM grades and at two MAM concentrations. Increasing the MAM molecular weight and the MAM content enhances nucleation and results in smaller cell sizes.

The results of this work prove that it is possible to produce nanocellular polymers based on PMMA without the need of a pressure pump or a heating system during the saturation stage, which is interesting for the possible production at industrial scale.

Declaration of Competing Interest

The authors declare that they have no known competing financial interests or personal relationships that could have appeared to influence the work reported in this paper.

Acknowledgments

Financial support from the FPU grant FPU14/02050 (V. Bernardo) from the Spanish Ministry of Education, Spain and the Junta of Castile and Leon grant (J. Martín-de León) are gratefully acknowledged. Financial assistance from the Spanish Ministry of Science, Innovation and Universities (RTI2018-098749-B-I00) are gratefully acknowledged. We would also like to thank Tolsa (Madrid, Spain) for supplying the sepiolites and Arkema for supplying the copolymers used in this research. Financial assistance from EREN (Ente Regional de la Energía de Castilla y León. EREN_2019_-L4_UVA) is gratefully acknowledged.

Appendix A. Supplementary data

Supplementary data to this article can be found online at https://doi.org/10.1016/j.matlet.2019.126551.

References

[1] L.J. Gibson, M. Ashby, Cellular Solids: Structure and Properties, 2nd ed., Cambridge University Press, 1997.
[2] D. Eaves, Handbook of Polymer Foams, Rapra Technology, United Kingdom, 2004.
[3] B. Notario, J. Pinto, M.A. Rodriguez-Perez, Nanoporous polymeric materials: a new class of materials with enhanced properties, Prog. Polym. Sci. 78–79 (2016) 93–139, https://doi.org/10.1016/j.pmatsci.2016.02.002.
[4] B. Notario, J. Pinto, E. Solorzano, J.A. de Saja, M. Dumon, M.A. Rodriguez-Perez, Experimental validation of the Knudsen effect in nanocellular polymeric foams, Polymer (Guildf). 56 (2015) 57–67, https://doi.org/10.1016/j.polymer.2014.10.006.
[5] C. Forest, P. Chaumont, P. Cassagnau, B. Swoboda, P. Sonntag, Polymer nanofoams for insulating applications prepared from CO 2 foaming, Prog. Polym. Sci. 41 (2015) 122–145, https://doi.org/10.1016/j.progpolymsci.2014.07.001.
[6] S. Liu, J. Duvigneau, G.J. Vancso, Nanocellular polymer foams as promising high performance thermal insulation materials, Eur. Polym. J. 65 (2015) 33–45, https://doi.org/10.1016/j.eurpolymj.2015.01.039.
[7] B. Notario, J. Pinto, M.A. Rodríguez-Perez, Towards a new generation of polymeric foams: PMMA nanocellular foams with enhanced physical properties, Polymer (Guildf). 63 (2015) 116–126, https://doi.org/10.1016/j.polymer.2015.03.003.
[8] D. Miller, V. Kumar, Microcellular and nanocellular solid-state polyetherimide (PEI) foams using sub-critical carbon dioxide II. Tensile and impact properties, Polymer (Guildf) 52 (2011) 2910–2919, https://doi.org/10.1016/j.polymer.2011.04.049.
[9] J. Martin-de Leon, V. Bernardo, M.A. Rodriguez-Perez, Key production parameters to obtain transparent nanocellular PMMA, Macromol. Mater. Eng. 1700343 (2017) 1–5, https://doi.org/10.1002/mame.201700343.
[10] S. Perez-Tamarit, B. Notario, E. Solorzano, M.A. Rodriguez-Perez, Light transmission in nanocellular polymers: are semi-transparent cellular polymers possible?, Mater Lett. 210 (2017) 39–41, https://doi.org/10.1016/j.matlet.2017.08.109.
[11] B. Notario, J. Pinto, R. Verdejo, M.A. Rodríguez-Pérez, Dielectric behavior of porous PMMA: from the micrometer to the nanometer scale, Polymer (Guildf). 107 (2016) 302–305, https://doi.org/10.1016/j.polymer.2016.11.030.
[12] B. Notario, A. Ballesteros, J. Pinto, M.A. Rodriguez-Perez, Nanoporous PMMA: a novel system with different acoustic properties, Mater. Lett. 168 (2016) 76–79, https://doi.org/10.1016/j.matlet.2016.01.037.
[13] H. Yokoyama, K. Sugiyama, Nanocellular structures in block copolymers with CO2-philic blocks using CO2 as a blowing agent: crossover from micro- to nanocellular structures with depressurization temperature, Macromolecules 38 (2005) 10516–10522, https://doi.org/10.1021/ma051757j.
[14] V. Kumar, N.P. Suh, A process for making microcellular parts, Polym. Eng. Sci. 30 (1990) 1323–1329, https://doi.org/10.1002/pen.760302010.
[15] J.E. Martini-Vvedensky, N.P. Suh, F.A. Waldman, United States Patent – MICROCELLULAR CLOSED CELL FOAMS AND THEIR METHOD OF MANUFACTURE, 4,473,665, 1984.
[16] J. Martin de-Leon, V. Bernardo, M.A. Rodriguez-Perez, Low density nanocellular polymers based on PMMA produced by gas dissolution foaming: fabrication and cellular structure characterization, Polymers (Basel) 8 (2016) 1–16, https://doi.org/10.3390/polym8070265.
[17] S. Costeux, S.P. Bunker, Homogeneous nanocellular foams from styrenic-acrylic polymer blends, J. Mater. Res. 17 (2013) 2351, https://doi.org/10.1557/jmr.2013.100.
[18] H. Guo, A. Nicolae, V. Kumar, Solid-state poly(methyl methacrylate) (PMMA) nanofoams. Part II: low-temperature solid-state process space using CO2 and the resulting morphologies, Polymer (Guildf). 70 (2015) 231–241, https://doi.org/10.1016/j.polymer.2015.06.031.
[19] K. Nadella, H. Guo, J. Weller, V. Kumar, Sorption and Desorption of CO 2 in Polycarbonate (PC) and Acrylonitrile Butadiene Styrene (ABS) in the Solid State Microcellular Process, (n.d.).
[20] C. Forest, P. Chaumont, P. Cassagnau, B. Swoboda, P. Sonntag, CO2 nanofoaming of nanostructured PMMA, Polymer (Guildf). 58 (2015) 76–87, https://doi.org/10.1016/j.polymer.2014.12.048.
[21] S. Costeux, L. Zhu, Low density thermoplastic nanofoams nucleated by nanoparticles, Polymer (Guildf). 54 (2013) 2785–2795, https://doi.org/10.1016/j.polymer.2013.03.052.
[22] S. Liu, B. Zoetebier, L. Hulsman, Y. Zhang, J. Duvigneau, G.J. Vancso, Nanocellular polymer foams nucleated by core-shell nanoparticles, Polymer (Guildf). 104 (2016), https://doi.org/10.1016/j.polymer.2016.09.016.
[23] S. Costeux, CO2-blown nanocellular foams, J. Appl. Polym. Sci. 131 (2014), https://doi.org/10.1002/app.41293.
[24] A. Alvarez, J. Santaren, A. Esteban-Cubillo, P. Aparicio, Development in Palygorskite-Sepiolite Research, Elsevier, 2011.
[25] J. Santaren, A. Alvarez, A. Esteban-Cubillo, B. Notario, D. Velasco, M.A. Rodrıguez-Perez, Improving the cellular structure and thermal conductivity of PS foams by using sepiolites 2012, in: Foams, 2012, pp. 1–5.
[26] V. Bernardo, J. Martin-de Leon, E. Laguna-Gutierrez, T. Catelani, J. Pinto, A. Athanassiou, M.A. Rodriguez-Perez, Understanding the role of MAM molecular weight on the production of PMMA/MAM nanocellular polymers, Polymer (Guildf.) 153 (2018) 262–270, https://doi.org/10.1016/j.polymer.2018.08.022.
[27] H. Guo, V. Kumar, Solid-state poly(methyl methacrylate) (PMMA) nanofoams. Part I: low-temperature CO2 sorption, diffusion, and the depression in PMMA glass transition, Polymer (Guildf). 57 (2015) 157–163, https://doi.org/10.1016/j.polymer.2014.12.029.
[28] J. Pinto, E. Solórzano, M.A. Rodriguez-Perez, J.A. De Saja, Characterization of the cellular structure based on user-interactive image analysis procedures, J. Cell. Plast. 49 (2013) 555–575, https://doi.org/10.1177/0021955X13503847.
[29] V. Bernardo, J. Martin-de León, E. Laguna-Gutiérrez, M.Á. Rodríguez-Pérez, PMMA-sepiolite nanocomposites as new promising materials for the production of nanocellular polymers, Eur. Polym. J. 96 (2017) 10–26, https://doi.org/10.1016/j.eurpolymj.2017.09.002.
[30] V. Bernardo, J. Martin-de Leon, J. Pinto, T. Catelani, A. Athanassiou, M.A. Rodriguez-Perez, Low-density PMMA/MAM nanocellular polymers using low MAM contents: production and characterization, Polymer (Guildf.) 163 (2019) 115–124, https://doi.org/10.1016/j.polymer.2018.12.057.
[31] V. Bernardo, J. Martin-de Leon, M.A. Rodriguez-Perez, Anisotropy in nanocellular polymers promoted by the addition of needle-like sepiolites, Polym. Int. 68 (2019) 1204–1214, https://doi.org/10.1002/pi.5813.
[32] S. Costeux, I. Khan, S.P. Bunker, H.K. Jeon, Experimental study and modeling of nanofoams formation from single phase acrylic copolymers, J. Cell. Plast. 51 (2015) 197–221, https://doi.org/10.1177/0021955X14531972.
[33] J. Pinto, M. Dumon, M. Pedros, J. Reglero, M.A. Rodriguez-Perez, Nanocellular CO2 foaming of PMMA assisted by block copolymer nanostructuration, Chem. Eng. J. 243 (2014) 428–435, https://doi.org/10.1016/j.cej.2014.01.021.
[34] J. Pinto, J.A. Reglero-Ruiz, M. Dumon, M.A. Rodriguez-Perez, Temperature influence and CO2 transport in foaming processes of poly(methyl methacrylate)–block copolymer nanocellular and microcellular foams, J. Supercrit. Fluids 94 (2014) 198–205, https://doi.org/10.1016/j.supflu.2014.07.021.
[35] C. Forest, P. Chaumont, P. Cassagnau, B. Swoboda, P. Sonntag, Nanofoaming of PMMA using a batch CO2 process: influence of the PMMA viscoelastic behaviour, Polymer (Guildf). 77 (2015) 1–9, https://doi.org/10.1016/j.polymer.2015.09.011.
[36] V. Realinho, M. Antunes, A.B. Martínez, J.I. Velasco, Influence of nanoclay concentration on the CO2 diffusion and physical properties of PMMA montmorillonite microcellular foams, Ind. Eng. Chem. Res. 50 (2011) 13819–13824, https://doi.org/10.1021/ie201532h.
[37] G. Wang, J. Zhao, L.H. Mark, G. Wang, K. Yu, C. Wang, C.B. Park, G. Zhao, Ultra-tough and super thermal-insulation nanocellular PMMA/TPU, Chem. Eng. J. 325 (2017) 632–646, https://doi.org/10.1016/j.cej.2017.05.116.